The *Salmonella* Typhimurium effector SteC inhibits Cdc42-mediated signaling through binding to the exchange factor Cdc24 in *Saccharomyces cerevisiae*

Pablo Fernandez-Piñar[a], Ainel Alemán[a], John Sondek[b], Henrik G. Dohlman[b], María Molina[a], and Humberto Martín[a]

[a]Departamento de Microbiología II, Facultad de Farmacia, Universidad Complutense de Madrid, and Instituto Ramón y Cajal de Investigaciones Sanitarias, 28040 Madrid, Spain; [b]Department of Pharmacology, University of North Carolina at Chapel Hill, Chapel Hill, NC 27599

ABSTRACT **Intracellular survival of *Salmonella* relies on the activity of proteins translocated into the host cell by type III secretion systems (T3SS). The protein kinase activity of the T3SS effector SteC is required for F-actin remodeling in host cells, although no SteC target has been identified so far. Here we show that expression of the N-terminal non-kinase domain of SteC down-regulates the mating and HOG pathways in *Saccharomyces cerevisiae*. Epistasis analyses using constitutively active components of these pathways indicate that SteC inhibits signaling at the level of the GTPase Cdc42. We demonstrate that SteC interacts through its N-terminal domain with the catalytic domain of Cdc24, the sole *S. cerevisiae* Cdc42 guanine nucleotide exchange factor (GEF). SteC also binds to the human Cdc24-like GEF protein Vav1. Moreover, expression of human Cdc42 suppresses growth inhibition caused by SteC. Of interest, the N-terminal SteC domain alters Cdc24 cellular localization, preventing its nuclear accumulation. These data reveal a novel functional domain within SteC, raising the possibility that this effector could also target GTPase function in mammalian cells. Our results also highlight the key role of the Cdc42 switch in yeast mating and HOG pathways and provide a new tool to study the functional consequences of Cdc24 localization.**

Monitoring Editor
Charles Boone
University of Toronto

Received: Mar 28, 2012
Revised: Jul 24, 2012
Accepted: Sep 18, 2012

INTRODUCTION

Salmonella are Gram-negative intracellular bacteria that cause diseases ranging from gastroenteritis to typhoid fever in humans and represent a major health problem worldwide (Ohl and Miller, 2001). These bacteria use type III secretion systems (T3SS) to deliver >30 *Salmonella* pathogenicity island (SPI)-1 and -2 effector proteins directly into the host cell cytosol (Galan and Wolf-Watz, 2006). These virulence factors enable the precise manipulation of key proteins for signaling and morphogenesis in the host. By these means, *Salmonella* cells induce their own internalization by nonphagocytic intestinal epithelial cells and are able to survive and replicate within this hostile environment. T3SS-1-delivered SPI-1 effectors are mainly required for bacterial entry into the nonphagocytic cells (Ly and Casanova, 2007). T3SS-2 is induced within host cells and delivers SPI-2-effectors important for the development of a modified phagosome called the *Salmonella*-containing vacuole (SCV), necessary for intracellular survival and favoring systemic spread (Steele-Mortimer, 2008). During systemic infection, macrophages represent an important site for replication of *Salmonella*, and T3SS-2 is essential for survival and multiplication within these immune cells (Chakravortty *et al.*, 2002). Furthermore, effectors secreted by both T3SS are involved in the modulation of inflammatory responses (McGhie *et al.*, 2009). Either proinflammatory or anti-inflammatory effects have been reported for different effectors, reflecting the complexity of the manipulation of host cell machinery orchestrated by this pathogen to secure its survival and proliferation.

This article was published online ahead of print in MBoC in Press (http://www.molbiolcell.org/cgi/doi/10.1091/mbc.E12-03-0243) on September 26, 2012.

Address correspondence to: María Molina (molmifa@farm.ucm.es).

Abbreviations used: CWI, cell wall integrity; GEF, guanine nucleotide exchange factor; HOG, high osmolarity glycerol; MAPK, mitogen-activated protein kinase; RGS, regulator of G protein signaling; T3SS, type III secretion system.

SCV biogenesis is an extremely dynamic process involving the formation of distinct tubular networks during host cell infection through extensive changes in intracellular membrane trafficking and actin cytoskeleton (Schroeder *et al.*, 2011). F-actin assembles in the vicinity of the SCV in the so-called vacuole-associated actin polymerizations, resulting in a nest or meshwork around bacteria clusters (Meresse *et al.*, 2001). The microtubule network and molecular motors also play an essential role in the formation of the membrane tubules called *Salmonella*-induced filaments in a process that involves the highly conserved Rho GTPase molecular switches (Bakowski *et al.*, 2008). Rho proteins play a key role in essential physiological processes such as signal transduction, membrane trafficking, and cytoskeletal dynamics (Heasman and Ridley, 2008). Targeting of cellular Rho GTPases occurs by *Salmonella* effectors that display guanine nucleotide exchange factor (GEF) or GTPase-activating protein (GAP) activities, mimicking the activity of mammalian counterparts and resulting in the modulation of the host cellular cytoskeleton and mitogen-activated protein kinase (MAPK) pathways that operate downstream. Effector proteins that post-translationally modify either Rho GTPases or their GEFs and GAPs also have been identified from distinct bacteria and shown to operate in the pathogenic process (Galan, 2009).

The ease of genetic manipulation, the availability of postgenomic tools, the wealth of biological knowledge, and the conservation of most cellular processes affected during bacterial infection in *Saccharomyces cerevisiae* have led to the emergence of this yeast as a very useful model for the study of bacterial virulence proteins (Rodríguez-Pachón *et al.*, 2002; Valdivia, 2004; Aleman *et al.*, 2005; Rodriguez-Escudero *et al.*, 2005). *S. cerevisiae* has six Rho GTPases, named Rho1–5 and Cdc42. Cdc42 plays a key role in the establishment of polarized growth by regulating the organization of the actin cytoskeleton. Cdc24 is the sole GEF controlling Cdc42 activity (Perez and Rincon, 2010). Moreover, Cdc24 seems to be essential for the localization of Cdc42 at the presumptive bud site on the plasma membrane and therefore for polarity establishment (Howell and Lew, 2012). This yeast also possesses five distinct signaling pathways involved in mating, pseudohyphal/invasive growth, cell wall integrity (CWI), osmoregulation, and ascospore formation, mediated by MAPKs Fus3, Kss1, Slt2, Hog1, and Smk1, respectively (Chen and Thorner, 2007). Fus3 and Kss1 are orthologues to mammalian extracellular signal-regulated kinase (ERK) 1/2, and Hog1 is orthologous to p38 (Caffrey *et al.*, 1999). The mammalian MAPK closest to Slt2 is ERK5 (Truman *et al.*, 2006). These MAPKs contain a highly conserved T-X-Y motif in the kinase activation loop in which both threonine and tyrosine residues must be phosphorylated to achieve kinase activation (Raman *et al.*, 2007).

The yeast mating pathway is one of the best-understood signaling routes in eukaryotes, and its study has produced important advances in elucidating components and mechanisms participating in MAPK signaling (Dohlman and Slessareva, 2006). This pathway is activated by binding of the mating pheromone to a cell surface receptor, which causes the dissociation of the heterotrimeric G-protein into Gα subunit (Gpa1) and the Gβγ dimer (Ste4–Ste18) complex. The GAP function of the RGS protein Sst2 promotes the reassociation of Gpa1 with Ste4–Ste18, eventually contributing to pathway adaptation and recovery. On dissociation of the G-protein, the Gβγ dimer helps to recruit the scaffold protein Ste5 to the plasma membrane, in complex with the MAPK kinase kinase (MAPKKK) Ste11, the MAPKK Ste7, and the MAPK Fus3, which phosphorylate one another in sequence. Activation of the first kinase of the cascade, Ste11, takes place at the plasma membrane through phosphorylation by its upstream activator, the PAK kinase Ste20, which in turn is activated by the small Rho GTPase Cdc42. In addition, Ste50 serves as an adaptor that links the Cdc42–Ste20 kinase complex to effector kinase Ste11. Once phosphorylated, the MAPK Fus3 translocates to the nucleus and phosphorylates Ste12, which activates transcription of pheromone response genes. The MAPK Kss1 is also transiently activated upon pheromone stimulation independently of the scaffold protein, Ste5. Some of the mating pathway components also participate in one of the two branches that lead to the activation of the MAPK Hog1. In the HOG pathway, Cdc42-dependent activation of Ste20 results in the sequential activation of the MAPKKK Ste11, the MAPKK Pbs2, and the MAPK Hog1. A number of distinct molecular mechanisms ensure that activated Ste11 does not transmit the signal to the MAPK Ste7 in response to a hyperosmotic shock, preventing spurious cross-talk between the HOG and mating pathways (Chen and Thorner, 2007).

In a previous report, we identified SteC in a genetic screen for *Salmonella* Typhimurium proteins that produce toxicity when overexpressed in the yeast model system (Aleman *et al.*, 2009). This protein was shown to be translocated into host cells in a T3SS-2–dependent manner, which led to its designation as *Salmonella* translocated effector C (SteC; Geddes *et al.*, 2005). SteC displays an incomplete but active catalytic protein kinase domain that is essential for SPI-2–dependent F-actin meshwork formation in host cells (Poh *et al.*, 2008). In the interest of identifying the cellular targets of this protein, we conducted a molecular and functional characterization of SteC in the model yeast *S. cerevisiae*. Here we show that the N-terminal region of SteC down-regulates the yeast MAPK mating pathway at the level of Cdc42. Binding experiments indicate that SteC targets both the yeast Cdc42 GEF Cdc24 and the human Cdc24-like protein Vav1. Therefore our data point to a role for SteC in the regulation of GTPase function in yeast, thereby laying the foundation for investigation of SteC activity in more complex mammalian systems.

RESULTS

SteC expression down-regulates signaling through the yeast mating pathway

SteC contains a region (spanning amino acids 230–280) displaying homology to protein kinases, with the closest similarity to the human RAF proto-oncogene serine/threonine kinase (Poh *et al.*, 2008; Aleman *et al.*, 2009). An activated N-terminally truncated version of the MAPKKK Raf1 has been shown to substitute for Ste11 in the yeast pheromone MAPK-mediated pathway (Irie *et al.*, 1994). With the aim of identifying the cellular targets of this protein, we used *S. cerevisiae* as a model to determine whether SteC was able to interfere with this pathway, by expressing SteC fused to glutathione *S*-transferase (GST) under the control of the inducible promoter *GAL1*.

Initially, we tested the effect of SteC expression on MAPK mating pathway signaling by a reporter transcription assay in which we used the pheromone-inducible *FUS1* promoter and *lacZ* (β-galactosidase) reporter gene. As shown in Figure 1A, expression of the bacterial effector greatly reduced the transcriptional response to pheromone, suggesting a negative regulatory effect on this pathway. Next we expressed SteC in *MATα itc1Δ* yeast cells, which display an autocrine constitutive stimulation of the mating pathway due to inappropriate secretion of **a**-factor (Figure 1B; Ruiz *et al.*, 2003). In this case, we analyzed the phosphorylation status of the MAPKs Fus3 and Kss1 using antibodies that detect the dually phosphorylated and thereby activated forms of MAPKs (Martin *et al.*, 2000). We first confirmed the identity of the distinct bands detected by these antibodies by activating the mating pathway in mutants lacking the

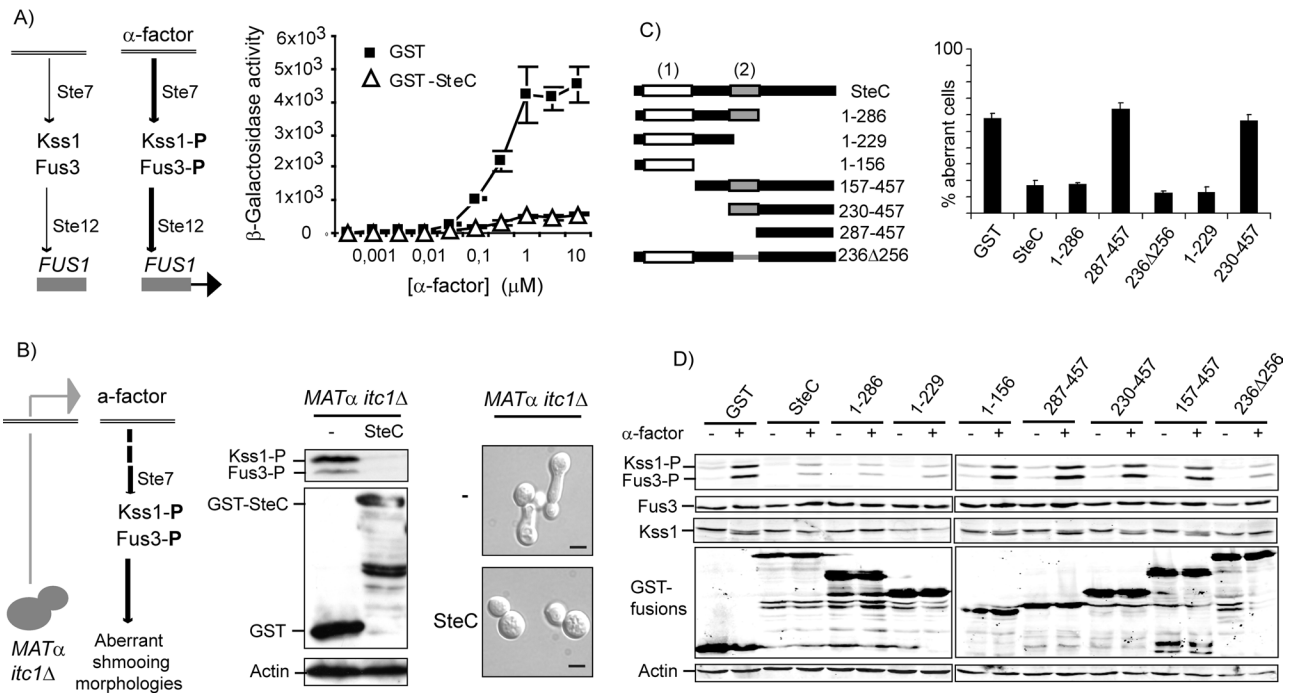

FIGURE 1: SteC inhibits signaling through the yeast pheromone response pathway. (A) Left, scheme illustrating pheromone stimulation of the mating pathway that results in Fus3 and Kss1 MAPK phosphorylation and Ste12-mediated *FUS1* transcriptional activation. Right, wild-type YPH499 cells bearing pEG(KG) or pEG(KG)-SteC plasmids, expressing GST or GST-SteC respectively, were transformed with the plasmid pRS423-FUS1-lacZ, containing the pheromone-inducible *FUS1* promoter and *lacZ* reporter gene. Cells were grown to mid–log phase in raffinose-based medium, with galactose added for a final 2% for 4 h, and then treated with the indicated concentration of α-factor for additional 90 min. β-Galactosidase activity was expressed as arbitrary fluorescence units. Data shown are the average of three independent experiments performed in triplicate. Error bars indicate standard deviations (SD). (B) Left, scheme illustrating how *MATα itc1Δ* yeast cells produce **a**-factor, leading to autocrine stimulation of the mating pathway. Middle, Western blotting analysis of cell extracts from the Y04500 *MATα itc1Δ* mutant strain transformed with the empty vector pEG-(KG) or pEG-(KG)-SteC, expressing GST or GST-SteC, respectively. Cells were grown as in A. Protein extracts were prepared, and the levels of phospho-Fus3 or phospho-Kss1, GST or GST fusions, and actin as loading control were detected by immunoblot analysis with anti–phospho-p44/42, anti-GST, and anti-actin antibodies, respectively. Right, DIC photographs showing the cell morphology of representative Y04500 *MATα itc1Δ* cells as in the middle. Bars, 5 μm. (C) Left, a schematic representation of the expressed fragments of SteC. The SteC region containing protein kinase subdomains is shown in gray, and the region showing similarity to RGS domains is indicated as white boxes. Right, percentage of cells displaying aberrant morphology from cultures of Y04500 *MATα itc1Δ* yeast cells expressing the indicated GST-tagged SteC fragments from pEG-(KG)–derived plasmids. Cells were observed 6 h after induction in galactose. Data are means of three experiments, and at least 100 cells were counted in each experiment. Error bars correspond to the SD. (D) Western blotting analysis of cell extracts from similar transformants as in C. Cells were cultured in absence (–) or presence (+) of 3 μM of α-factor, and protein extracts were prepared and analyzed as in B. Fus3 and Kss1 were detected with anti-Fus3 and anti-Kss1 antibodies, respectively. Reproducible results were obtained in different experiments, and selected images correspond to representative blots.

targeted MAPKs (Supplemental Figure S1). As observed in Figure 1B, the expression of GST-SteC resulted in a drastic reduction of the amount of phospho-Kss1 and phospho-Fus3 compared with control cells expressing GST. SteC also reduced the aberrant cell morphology of *MATα itc1Δ* yeast cells, which resemble the polarized mating projection of cells responding to pheromone. These results clearly indicate that SteC negatively regulates the yeast mating pathway upstream of the MAPKs.

To establish the domain of SteC responsible for this inhibitory effect on signaling, we constructed a series of plasmids expressing distinct regions of SteC as GST fusions under the *GAL1* promoter (Figure 1C). Western blotting analysis confirmed that all these SteC-derived proteins were correctly expressed (Figure 1D). Galactose-dependent production of the C-terminal domain of SteC ($SteC^{230-457}$) including the kinase region neither reduced the percentage of MATα *itc1Δ* cells displaying aberrant morphology (Figure 1C) nor resulted in a decrease of Fus3 and Kss1 phosphorylation after pheromone stimulation (Figure 1D). The shorter $SteC^{287-457}$ construct, which excludes the kinase region, did not result in signaling inhibition. In contrast, expression of the N-terminal fragment of SteC, either bearing ($SteC^{1-286}$) or lacking ($SteC^{1-229}$) the kinase region, led to a reduced pathway output (Figure 1, C and D). A similar inhibitory effect was obtained when expressing a version of SteC in which amino acids 236–256 were deleted and thus just lacking the kinase domain. Of interest, expression of either a shorter N-terminal fragment of SteC ($SteC^{1-156}$) or SteC lacking these first 156 amino acids did not alter signaling (Figure 1D). We also observed that phosphorylation of Kss1 increased its electrophoretic mobility. Accordingly, disappearance of the faster Kss1 band only occurred in samples from cells expressing full-length SteC or SteC fragments with inhibitory activity

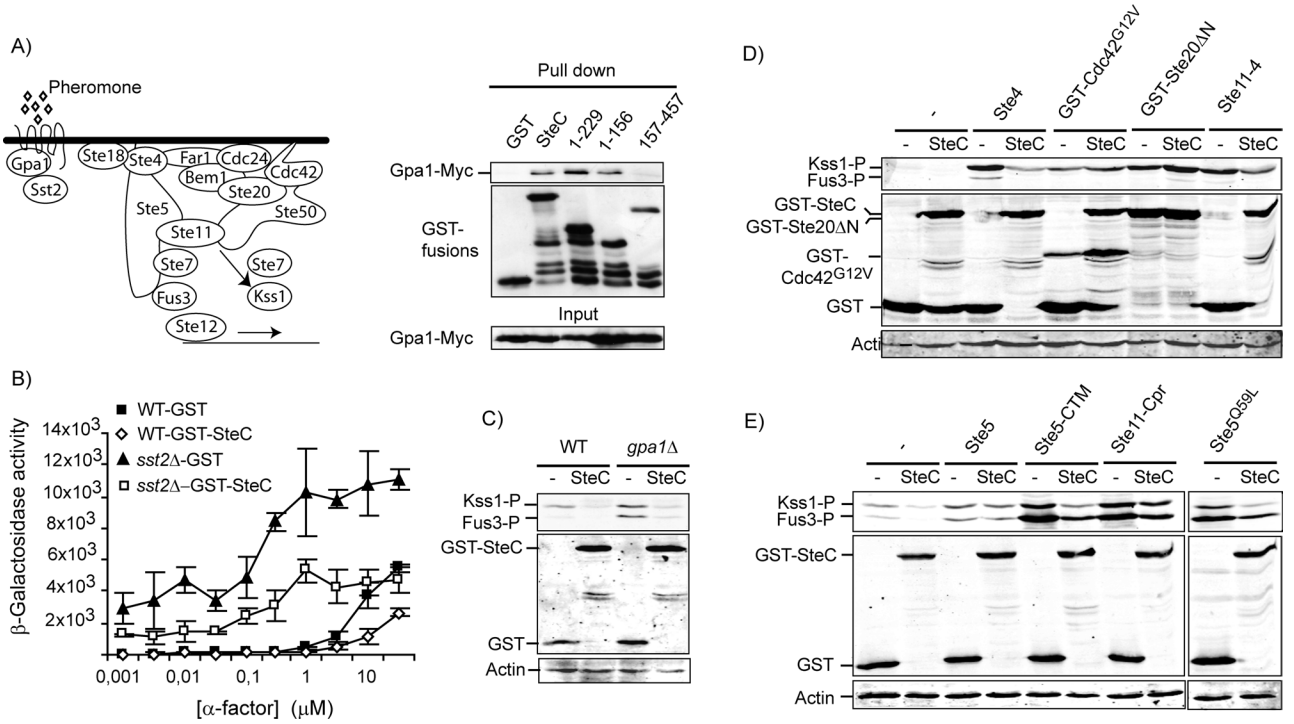

FIGURE 2: SteC binds Gpa1 but acts in the mating pathway independently of both the G_α subunit and the MAPK module. (A) Left, main components that operate in the yeast mating pathway. Right, immunoblot analysis of the copurification of Gpa1-6Myc with the indicated GST-tagged SteC fragments. Transformants of the YPH499 (*GPA1-6Myc*) strain with the plasmids pEG(KG) (GST), pEG-(KG)-SteC (SteC), pEG-(KG)-SteC$^{1\text{-}229}$ (1–229), pEG-(KG)-SteC$^{1\text{-}156}$ (1–156), or pEG-(KG)-SteC$^{157\text{-}457}$ (157–457) were grown to mid–log phase in raffinose-based selective medium and then galactose was added for a final 2% for an additional 6 h. Cell extracts (input) and GST complexes obtained by purification with glutathione-Sepharose (pull down) were analyzed by immunoblotting with anti-Myc and anti-GST antibodies. (B) Transcription activity in response to distinct α-factor concentrations was measured as indicated in Figure 1A in strains YPH499 (WT) and YDM400 (*sst2*Δ) bearing the plasmid pRS423-FUS1-lacZ and transformed with pEG(KG) or pEG(KG)-SteC plasmids. Data shown are the average of three independent experiments performed in triplicate. Error bars indicate standard deviations. (C) Western blotting analysis of cell extracts from BY4741 (WT) and BYgpa1 (*gpa1*Δ) strains transformed with the empty vector pEG-(KG) or pEG-(KG)-SteC expressing GST (–) or GST-SteC (SteC), respectively. Cells were cultured and cell extracts analyzed as in Figure 1B. (D) Western blotting analysis of cell extracts from YPH499 (WT) cells expressing GST (–) or GST-SteC (SteC) from pEG-(KG)–derived plasmids and transformed with empty vector pEG(KG)H (–) or plasmids pRS315-GAL-*STE4*, pEG(KG)H-*cdc42*^{G12V}, and pRS425-*ste11-4* in order to overproduce Ste4 or the corresponding hyperactive versions of Cdc42 and Ste11-4. In the case of cells bearing pEG(KG)-*ste20ΔN*, which overproduce the corresponding hyperactive version of Ste20, SteC was expressed from plasmid YCpLG-SteC. Cells were cultured and extracts were analyzed as in Figure 1B. (E) Western blotting analysis of cells extracts from YPH499 (WT) cells expressing GST (–) or GST-SteC (SteC) from pEG-(KG)–derived plasmids and transformed with empty vector pRS316GAL or plasmid pGFP-G-STE5, pG-STE5-CTM, pT-G-STE11-Cpr, or pCUGF-STE5Q59L. Cells were cultured and extracts were processed and analyzed as in Figure 1B.

on the mating pathway. In sum, these data indicate that the N-terminal region spanning the first 229 amino acids is necessary for the SteC-induced inhibitory effect on signaling through the mating pathway, which is independent of SteC kinase activity.

SteC acts upstream of the mating MAPK module and independently of the G_α subunit Gpa1

Our structural analysis within the SteC N-terminal region using the SMART domain search tool identified a region encompassing amino acids 18–156 with low similarity to Regulator of G Protein Signaling (RGS) domains. Given that a receptor-coupled heterotrimeric G protein participates in the yeast mating pathway (Figure 2A), this finding suggested that SteC could act on the α subunit Gpa1 in a manner similar to the RGS protein Sst2, which down-regulates the mating pathway by promoting the GTPase activity of Gpa1 (Apanovitch *et al.*, 1998). Consistent with this hypothesis, GST-SteC through the first 156 amino acids was able to pull down Gpa1-Myc from yeast cell extracts (Figure 2A). We next used the reporter transcription assay based on the *FUS1* promoter to analyze the effect of expressing SteC in an *sst2*Δ mutant strain (Dohlman *et al.*, 1995). As observed in Figure 2B, deletion of the RGS-coding gene *SST2* resulted in increased sensitivity (EC_{50}) and maximum response to pheromone, as well as an increase in the basal activity of the pathway. Although overexpression of SteC reduced both basal signaling and maximum responsiveness of this mutant, it failed to restore the EC_{50} to wild-type levels (Figure 2B), suggesting that SteC is acting by using a different mechanism than the RGS Sst2. Furthermore, deletion of *GPA1* did not prevent the down-regulating activity of SteC on Fus3 and Kss1 phosphorylation (Figure 2C), clearly indicating that SteC acts in a Gpa1-independent manner.

To map the position in which SteC was impinging on the pheromone signaling pathway, we investigated the effect of SteC on

MAPK phosphorylation in strains in which the pathway was constitutively activated from distinct points of the signaling cascade, namely by overexpression of the G protein β subunit Ste4 (Cole *et al.*, 1990), the GTP-bound Cdc42^{G12V} version (Andersson *et al.*, 2004), an N-terminally truncated version of Ste20 lacking the kinase-inhibitory CRIB domain (Ste20ΔN; Ramer and Davis, 1993; Martin *et al.*, 1997), or the hyperactive MAPKKK version Ste11-4 (Stevenson *et al.*, 1992). As shown in Figure 2D, SteC reduced signaling resulting from overexpression of Ste4, confirming that SteC targets elements downstream the G protein α subunit. In contrast, SteC did not inhibit signaling in cells producing either Cdc42^{G12V} or Ste20ΔN. These results indicate that SteC is not acting on the Ste11-Ste7-Fus3/Kss1 MAPK cascade but instead on one of the upstream components. The weak SteC-induced reduction of signaling observed when expressing Ste11-4 is compatible with this model because Ste11-4 is still regulated by phosphorylation and therefore is able to transmit signaling from upstream elements (Drogen *et al.*, 2000). The lack of effect on the Ste20ΔN-induced activation of the pathway suggests that SteC is not directly affecting Ste20 kinase activity. On the basis of these data, SteC is likely acting on one of the early steps of the mating pathway, for example, by interfering with either the Ste5-dependent recruitment of the kinase cascade to the plasma membrane or the Cdc42-promoted Ste20 activation.

To test the first possibility, we analyzed the effect of SteC overexpression on the constitutive activation caused by artificial targeting of the Ste5 scaffold or the Ste11 MAPKKK to the plasma membrane, which occurs in a heterotrimeric G protein–independent manner. To this end, we measured MAPK phosphorylation in cells expressing Ste5^{Q59L} or Ste5-CTM versions localized at the membrane via an enhanced PM domain (Winters *et al.*, 2005) or a foreign transmembrane domain (Pryciak and Huntress, 1998), respectively. We also used the Ste11-Cpr version targeted to the membrane via a prenylation/palmitoylation motif (Winters *et al.*, 2005). In all cases, overproduction of SteC led to a reduction in MAPK activation (Figure 2E), indicating that SteC is not interfering with the membrane recruitment mediated by Ste5. Furthermore, these results rule out the possibility that SteC acts on the heterotrimeric G protein.

Next we checked whether the lack of other proteins involved in the initial steps of mating signaling, like the scaffold proteins Bem1 and Far1 (Cote *et al.*, 2011) and the Ste11 adaptor Ste50 (Truckses *et al.*, 2006), affected the SteC-induced reduction of MAPK phosphorylation. Deletion of either *BEM1* or *FAR1* does not impede signaling through the pathway. However, to analyze the effect of SteC in a *ste50*Δ mutant, cells carried a version of Ste5 (Ste5^{Q59L}) that bypasses the requirement of Ste50 for mating signaling (Pryciak and Huntress, 1998; Winters *et al.*, 2005). The inhibitory effect of SteC was observed in all cases (unpublished data), indicating that Bem1, Far1, and Ste50 are not targets for SteC.

As described, SteC inhibits pathway activation by pheromone but not by the constitutively active mutant Cdc42^{G12V}. We also determined the effect of SteC on cells expressing Cdc42^{G12V} and treated with α-factor. Pheromone stimulation strongly increases Cdc42^{G12V}-mediated activation of the pathway (Supplemental Figure S2). However, SteC expression was also unable to reduce MAPK phosphorylation under these conditions. These data suggest that SteC acts on Cdc42 function.

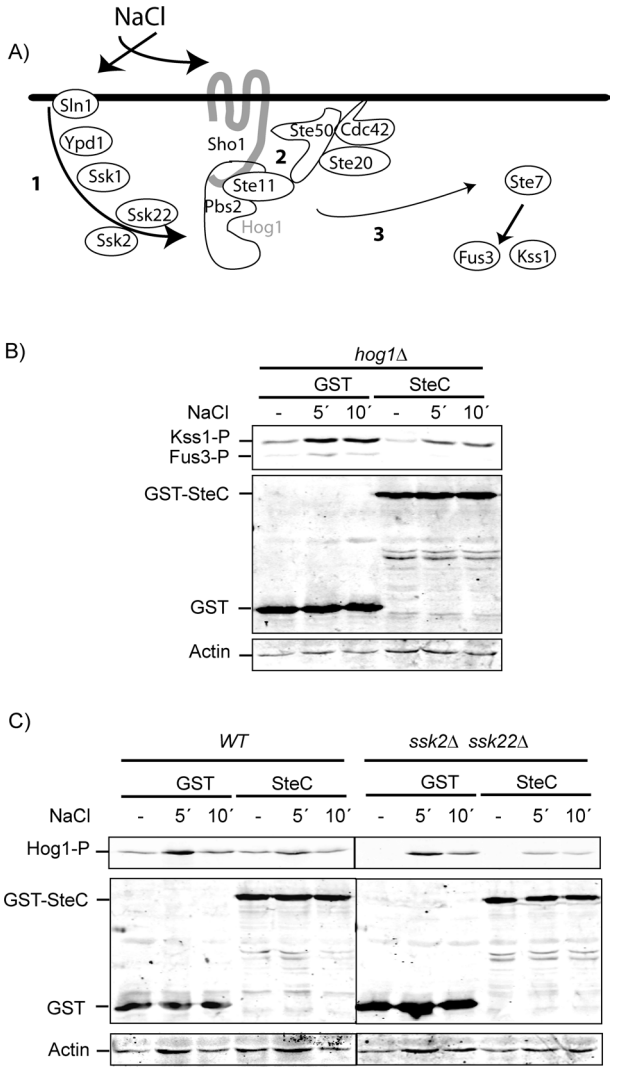

FIGURE 3: SteC inhibits signaling through the Cdc42-dependent branch of the HOG pathway. (A) Scheme illustrating the main components that operate in the HOG pathway, including the Sln1-mediated (1) and Sho1-mediated (2) branches of the pathway and the cross-talk that takes place in the absence of Hog1 (3), leading to the spurious phosphorylation of mating MAPKs after high salt stress. (B) Western blotting analysis of cell extracts from the Y02724 (*hog1*Δ) strain bearing the empty vector pEG-(KG) or pEG-(KG)-SteC, expressing GST or GST-SteC, respectively. Cells were grown to mid–log phase in raffinose-based selective medium, galactose was added for a final 2% for additional 6 h, and then cells were treated with 0.7 M NaCl for the indicated number of minutes. Protein extracts were prepared and analyzed as in Figure 1B. (C) Western blotting analysis of cell extracts from the TM141 (WT) and the TM257 (*ssk2*Δ *ssk22*Δ) strains bearing the empty vector pEG-(KG) or pEG-(KG)-SteC. Cells were cultured and extracts were processed and analyzed as in Figure 1B. The level of phospho-Hog1 was detected with anti–phospho-p38 antibodies. Reproducible results were obtained in different experiments, and selected images correspond to representative blots.

SteC prevents cross-talk between the HOG and pheromone response MAPK pathways in *hog1*Δ cells

It has been described that the MAPK Hog1 prevents cross-talk between the HOG and the pheromone response pathways (O'Rourke and Herskowitz, 1998). Thus the lack of Hog1 allows osmolarity-induced activation of the pheromone MAPK cascade in a process that is dependent on the Cdc42 node but independent of other components of the mating pathway (Figure 3A). As observed in Figure 3B, overexpression of SteC reduces the NaCl-induced phosphorylation of mating MAPKs in a *hog1*Δ strain, suggesting that

SteC is acting on a component shared by this cross-talk circuit and the mating pathway, possibly Cdc42. In accordance with these results, SteC was also able to reduce signaling through the HOG pathway in response to high salt stress, as determined by a decrease in Hog1 phosphorylation (Figure 3C). This inhibitory effect of the bacterial effector was magnified in a strain lacking Ssk2/22. In this case one of the two inputs to the HOG pathway is missing, leaving only the HOG branch that is mediated by Cdc42 (Figure 3C). Taken together, these data strongly support the idea that SteC acts as a negative regulator of Cdc42-mediated signaling.

Cdc42 overexpression rescues SteC-induced inhibition of yeast growth

We previously showed that overexpression of either full-length or the N-terminal region of SteC in yeast cells leads to strong growth inhibition (Aleman *et al.*, 2009). Therefore overexpression of the yeast SteC target is expected to relieve the lack of growth induced by this bacterial effector. Therefore, as a parallel and complementary approach to the epistasis analysis, we performed a genetic screen searching for suppressors of SteC toxicity. To this end, we transformed a *GAL1*-driven yeast cDNA library in cells overexpressing *steC* under the same promoter and selected clones able to grow on galactose-inducing conditions. All positive clones shared the same DNA insert corresponding to yeast *CDC42* (Figure 4A). Human Cdc42 is known to functionally replace its yeast orthologue (Munemitsu *et al.*, 1990). Accordingly, overexpression from a different *GAL1*-based plasmid of either yeast or human *CDC42* also overcame SteC toxicity (Figure 4A). Moreover, overexpression of yeast proteins related to Cdc42 function, such as Cdc43, Gic2, Rho3, Rsr1, and Ste20, which have been shown to compensate growth defects of distinct defective alleles of *CDC42* (Kozminski *et al.*, 2000, 2003), also alleviated SteC toxicity to a distinct extent (Supplemental Figure S3). Taken together, these results confirm that SteC-induced growth defects are caused by inhibition of Cdc42 function and are in agreement with the observed effects on the mating pathway.

To carry out cellular localization studies, we tagged SteC with green fluorescent protein (GFP). Fluorescence microscopy observations revealed that SteC-GFP predominantly showed peripheral localization, likely associated to the plasma membrane, but also colocalized with the marker FM4-64 that stains vacuolar and endosome membranes (Vida and Emr, 1995; Figure 4B). SteC$^{1-229}$ presented the same localization as the full-length SteC, whereas SteC$^{157-457}$ showed a cytoplasmic distribution in the cells (Figure 4C), indicating that the N-terminal part of the protein is responsible for membrane targeting. GFP-Cdc42 also localized associated to membranes either in the presence or the absence of SteC (Figure 4C). Moreover, we analyzed the presence of phosphoinositides phosphatidylinositol 4,5-bisphosphate and phosphatidylinositol 4-phosphate in yeast cells overexpressing SteC. These lipids are important for recruitment of proteins that contain phosphoinositide-binding domains (Strahl and Thorner, 2007) and play a role in Cdc42 functionality (Yakir-Tamang and Gerst, 2009). SteC expression did not alter the cellular distribution of these phosphoinositides, as detected by using specific fluorescent probes (Stefan *et al.*, 2002; Supplemental Figure S4). These data ruled out that mislocalization of Cdc42 or phosphoinositides alteration is the cause of the Cdc42 functional defect induced by SteC.

SteC physically interacts with Cdc24, the sole GEF for Cdc42

To determine whether SteC binds Cdc42, we carried out copurification experiments with yeast cells coexpressing GST-SteC and either

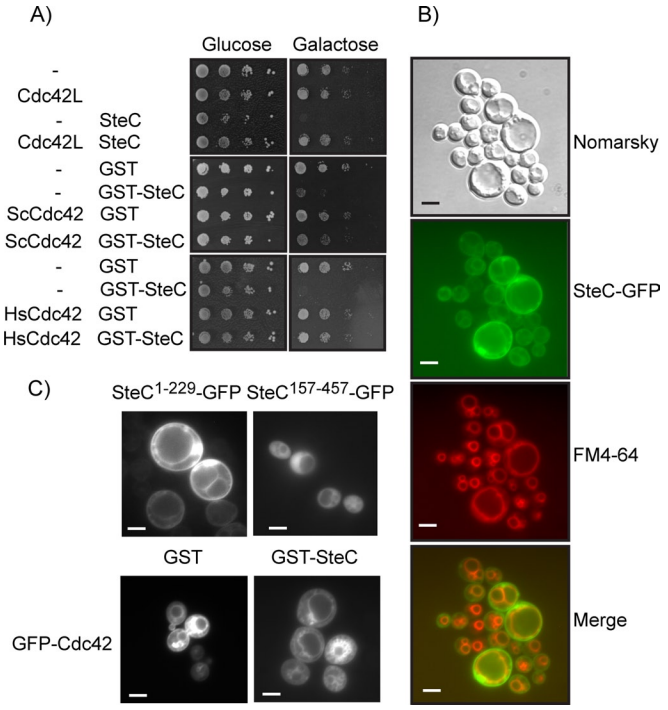

FIGURE 4: (A) Growth on SD (glucose) and SG (galactose) plates of serial dilutions of wild-type YPH499 yeast cells harboring the following plasmids, as indicated: YCpLG (–), YCpLG-SteC (SteC), pEG(KG) (GST), pEG(KG)-SteC (GST-SteC), pYES2 (–), pYES2-Cdc42-L (Cdc42-L), BG1805-Cdc42 (ScCdc42), and pYES2-HsCdc42 (HsCdc42), and therefore expressing under the control of the *GAL1* promoter the corresponding proteins on galactose-based medium. (B) DIC and fluorescence microscopy photographs showing the cell morphology (Nomarski), SteC-GFP localization, and internal membrane localization (FM4-64) of YPH499 strain harboring the plasmid pGFP-CFUS-SteC expressing SteC-GFP. Cells were grown to mid–log phase in complete SD medium, washed, and then transferred to SD medium lacking methionine for 6 h and then treated with the vacuolar–membrane staining FM464. Bars, 5 µm. (C) Top, fluorescence microscopy photographs showing the in vivo localization of SteC$^{1-229}$ and SteC$^{1-157}$. YPH499 cells transformed with either pGFP-CFUS-SteC$^{1-229}$ or pGFP-CFUS-SteC$^{1-157}$ were grown to mid–log phase in complete SD medium and transferred to a SD medium lacking methionine for 6 h. Bottom, fluorescence microscopy photographs showing the in vivo localization of GFP-Cdc42 in cells expressing GST or GST-SteC, as indicated. YPH499 cells bearing pRS415-GFPCDC42 and pEG-KG or pEG-KG-SteC were grown to mid–log phase in raffinose-based selective medium lacking methionine, and then galactose was added for a final 2% for additional 6 h. Bars, 5 µm.

yeast or human hemagglutinin (HA)-tagged versions of Cdc42. The negative-dominant HsCdc42^{T17N} (Feig, 1999) and the constitutively active HsCdc42^{G12V} versions were also tested for their ability to bind SteC. No interaction was detected between SteC and any of these Cdc42 mutant proteins (Figure 5A and unpublished data). In contrast, the *Salmonella* mutant effector SopB^{R468A}, known to interact with Cdc42 (Rodriguez-Escudero *et al.*, 2011), pulled down human Cdc42 (Figure 5A). Both yeast two-hybrid and in vitro copurification assays with recombinant proteins expressed in *Escherichia coli* were also negative for interaction between SteC and Cdc42 (unpublished data).

Activation of yeast Cdc42 relies on its sole GEF protein, Cdc24. This GEF controls Cdc42 function, and therefore *cdc24* mutants display the same phenotype as loss-of-function *cdc42* mutant cells

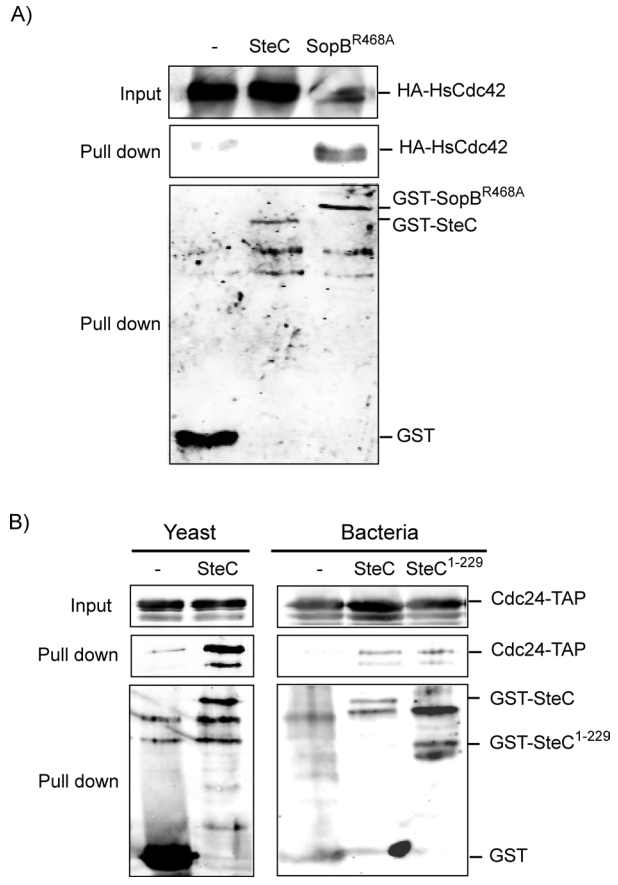

FIGURE 5: SteC interacts with the Cdc42 GEF Cdc24. (A) Copurification assays of HA-HsCdc42 with GST (–), GST-SteC (SteC), or GST-SopB^{R468A}. Transformants of the YPH499 strain with plasmid pYES3HA-Cdc42 and pEG(KG) (–), pEG(KG)-SteC (SteC), or pEG(KG)-SopB^{R468A} (SigD^{R468A}) were grown to mid–log phase in raffinose-based selective medium, and then galactose was added for a final 2% for an additional 6 h. Cell extracts (input) and GST complexes obtained by precipitation with glutathione-Sepharose (pull down) were analyzed by immunoblotting with anti-HA and anti-GST antibodies as indicated. (B) Copurification assays of Cdc24-TAP with, as indicated, either yeast- or *E. coli*–produced GST (–), GST-SteC (SteC), or GST-SteC$^{1-229}$ (SteC$^{1-229}$). For yeast expression, transformants of the YPH499 strain with plasmid BG1805-Cdc24 and pEG(KG) (–), pEG(KG)-SteC (SteC), or pEG(KG)- SteC$^{1-229}$ (SteC$^{1-229}$) were grown to mid–log phase in raffinose-based selective medium, and then galactose was added for a final 2% for an additional 6 h. Cell extracts (input) and GST complexes obtained by precipitation with glutathione-Sepharose (pull down) were analyzed by immunoblotting with anti-TAP and anti-GST antibodies as indicated. For in vitro copurification assays of recombinant SteC, *E. coli* extracts containing GST, GST-SteC, or GST-SteC$^{1-229}$ were incubated with yeast extracts containing Cdc24-TAP and glutathione-Sepharose to pull down GST complexes. Immunodetection was performed using anti-TAP (top) and anti-GST (bottom) antibodies. Reproducible results were obtained in different experiments, and selected images correspond to representative blots.

(Perez and Rincon, 2010). Thus SteC could be inhibiting Cdc42 function by targeting its positive regulator. To test this, we analyzed binding of SteC to Cdc24. As shown in Figure 5B, interaction experiments in yeast revealed that tandem affinity purification–tagged Cdc24 copurified with GST-SteC. Moreover, both *E. coli*–produced recombinant GST-SteC and Gst-SteC$^{1-229}$ were also able to pull down Cdc24 (Figure 5B). These data evidenced that the N-terminal region of SteC interacts with Cdc24, likely resulting in the inhibition of Cdc42 function.

SteC binds to *Schizosaccharomyces pombe* and human Cdc24 homologues

The use of the yeast model led us to identify Cdc24 as a target of SteC. Then we wanted to know whether SteC was able to bind similar GEFs from other organisms, including human, the natural host of *Salmonella*. We first tested interaction with *Schizosaccharomyces pombe* Scd1, the Cdc42 GEF homologue to Cdc24 (Perez and Rincon, 2010), by copurification experiments using a HA-tagged version of this protein. As shown in Figure 6A, *E. coli*–produced recombinant GST-SteC was able to pull down HA-Scd1 from *S. pombe* extracts. Therefore the ability of SteC to bind Cdc42 GEFs is extended to evolutionary distant yeast like the fission yeast *S. pombe*. Of interest, no binding of SteC to Rom1, a GEF for *S. cerevisiae* Rho1 GTPase, was observed (unpublished data). This is consistent with the lack of inhibitory effect of SteC on the cell integrity MAPK pathway mediated by Rho1 (Aleman *et al.*, 2009).

Like other Dbl-family GEFs (Rossman *et al.*, 2005), *S. cerevisiae* Cdc24 has a catalytic Dbl homology (DH) domain responsible for the GEF activity. The fact that sequence similarity between Cdc24 and Scd1 mainly occurs within their DH domains (31% identity) led us to examine whether SteC interacted with this domain of Cdc24. To this end, we looked at the ability of GST-SteC to pull down the DH domain of Cdc24 (Cdc24$^{287-473}$) tagged to Myc. As shown in Figure 6B, both full-length Cdc24-Myc and Cdc24 (DH)-Myc copurified with GST-SteC. These results indicate that the SteC *Salmonella* effector is likely to target GEFs through binding to the catalytic DH domain.

Next we tested the interaction of SteC with Vav1, one of the members of the human Dbl family of Rho GEFs that displays significant similarity at the catalytic DH domain to yeast Cdc24 (24% identity). Vav1 activates Cdc42, Rac1, and RhoA GTPases and is involved in key biological functions, including actin cytoskeleton reorganization and activation of ERK and Jun N-terminal kinase, as well as development and activation of immune cells (Lazer and Katzav, 2011). Copurification in vitro assays with recombinant *E-coli*–produced proteins showed that both GST-SteC and GST-Cdc42, used as a positive control, were able to bind the polyhistidine (polyHis)-tagged DH domain of the human GEF Vav1 (Figure 6C). Moreover, the N-terminal fragment of SteC (SteC$^{1-229}$) also pulled down the DH domain of Vav1. These results suggest that SteC binding to the DH domain of GEFs might interfere with the corresponding Rho GTPase function in *Salmonella*-infected cells. Although the most plausible mechanism underlying this effect would be the inhibition of the catalytic activity of the GEF, in vitro assays showed that neither GST-SteC nor GST-SteC$^{1-229}$ altered the exchange ability of Vav1 toward Rac1, the GTPase to which Vav1 GEF activity is most effective (Rapley *et al.*, 2008; Figure 6D).

SteC prevents nuclear localization of Cdc24

Our results suggested that SteC does not inhibit the catalytic activity of bound GEF. To investigate how this effector could be altering GEF function, we analyzed several known layers of regulation of Cdc24, namely phosphorylation, oligomerization, and spatial regulation. The PAK kinase Cla4 has been shown to phosphorylate Cdc24, leading to a mobility shift in SDS–PAGE (Gulli *et al.*, 2000; Bose *et al.*, 2001). As shown in Figure 7A, SteC does not inhibit phosphorylation of Cdc24 caused by the expression of a constitutively active version of Cla4 (Martin *et al.*, 1997).

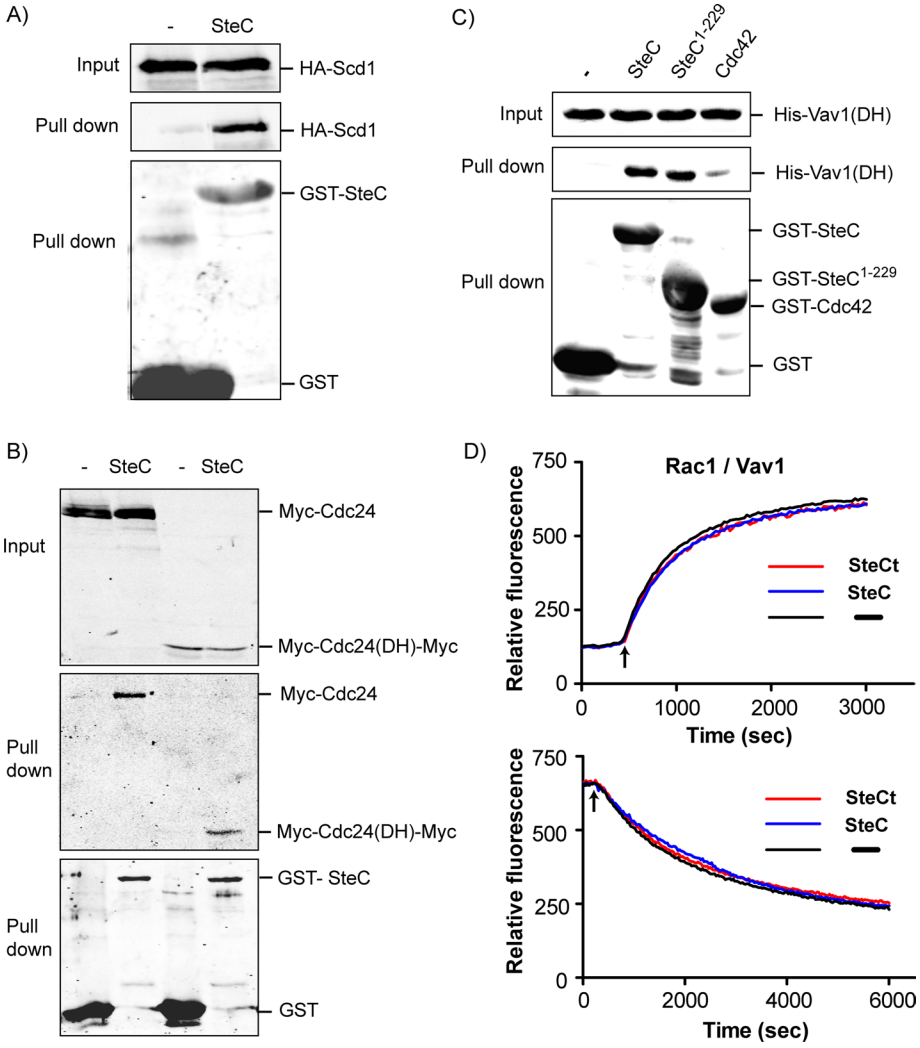

FIGURE 6: SteC binds *S. pombe* Scd1 and human Vav1 GEFs. (A) Copurification assays of HA-Scd1 with recombinant GST (–) or GST-SteC (SteC). *E. coli* extracts containing GST or GST-SteC were incubated with *S. pombe* extracts containing HA-Scd1 and glutathione-Sepharose to pull down GST complexes. Immunodetection was performed using anti-HA (top) and anti-GST (bottom) antibodies. (B) Copurification assays of Myc-Cdc24 and Myc-tagged Cdc24$^{287\text{-}473}$ (Cdc24(DH)) with GST (–) or GST-SteC (SteC). Transformants of the YPH499 strain with plasmid p414-3xmycCdc24Fl or p414-3xmycDH-3xmyc and pEG(KG) (–) or pEG-(KG)-SteC (SteC) were grown to mid–log phase in raffinose-based selective medium, and then galactose was added for a final 2% for an additional 6 h. Cell extracts (input) and GST complexes obtained by precipitation with glutathione-Sepharose (pull down) were analyzed by immunoblotting with anti-Myc and anti-GST antibodies as indicated. (C) Copurification assays of the DH domain of human Vav1 with recombinant GST (–), GST-SteC (SteC), GST-SteC$^{1\text{-}229}$ (SteC$^{1\text{-}229}$), or GST-Cdc42. *E. coli* extracts containing GST or GST-fused proteins were incubated with *E. coli* extracts containing His-tagged Vav1(DH) and glutathione-Sepharose to pull down GST complexes. Immunodetection was performed using anti-His (top) and anti-GST (bottom) antibodies. Reproducible results were obtained in different experiments, and selected images correspond to representative blots. (D) Purified SteC does not modulate the Vav1-catalyzed exchange of guanine nucleotides bound to Rac1. Top, purified Rac1 (400nM) was incubated with Bodipy FL GDP (80 nM) before addition (arrow) of Vav1 preincubated with indicated forms of SteC. Final concentrations of Vav1 and SteC were 5 and 50 nM, respectively. Bottom, purified Rac1 (400 nM) preloaded with Bodipy FL GDP was incubated with excess GDP (20 μM) before addition (arrow) of Vav1 preincubated with indicated forms of SteC. Final concentrations of Vav1 and SteC were 10 and 100 nM, respectively.

It is also known that Cdc24 shuttles between the nucleus and sites of cell growth. Cdc24 accumulates in the nucleus during late M phase and early G1 phase but then localizes at the incipient bud site during G1 phase, the bud tip at S and G2–M phases, and the mother–daughter bud neck during M phase (Toenjes *et al.*, 1999). To investigate whether SteC affects the localization of this GEF, we examined GFP-Cdc24 localization in cells expressing GST, GST-SteC, or GST-SteC$^{1\text{-}229}$. As expected, Cdc24 localized to the nucleus in unbudded and small-budded control cells after 6 h of galactose-induced expression of GST (Figure 7B). Remarkably, the expression of GST-SteC clearly reduced the percentage of cells with nuclear Cdc24 (to 15%, down from 32% in control GST-expressing cells). Nuclear Cdc24 was reduced further to just 1% of cells expressing the SteC N-terminal domain (Figure 7C). Western blotting analysis revealed that the amount of GFP-Cdc24 was similar in cells expressing either GST or SteC-derived GST fusion proteins (Figure 7D), indicating that the alteration of Cdc24 nuclear localization was not due to degradation of the protein. Oligomerization regulates subcellular localization of Cdc24 (Mionnet *et al.*, 2008). As observed in Figure 7E, however, SteC did not alter the amount of Cdc24-HA bound to Myc-Cdc24 in yeast coimmunoprecipitation experiments, ruling out the inhibition of Cdc24 oligomerization as the mechanism underlying the observed localization defects.

As expected, after 6 h of galactose induction, SteC- or SteC$^{1\text{-}229}$-expressing cells became big and round, and thus it was not possible to follow Cdc24 localization at different cell-cycle stages. To overcome this limitation, we carried out a Cdc24 localization analysis with cells after just 2 h of galactose-induced expression of GST or SteC-derived GST-fusion proteins, in which GFP-Cdc24 production was confirmed by Western blotting (Figure 7H). Consistent with data presented in Figure 7C, whereas a high percentage of control cells expressing GST showed Cdc24 in the nucleus at G1 or M phase, a reduction of nuclear Cdc24 was observed in cells expressing SteC. Expression of SteC$^{1\text{-}229}$ completely prevented nuclear Cdc24 in cells at these stages (Figure 7, F and G). In addition, the percentage of cells displaying Cdc24 localization at polarized growth sites was also reduced upon expression of either SteC or SteC$^{1\text{-}229}$, although this effect was milder than that observed for nuclear Cdc24 localization (Figure 7G). Taken together, these results indicate that Cdc24 localization is significantly altered by SteC expression.

DISCUSSION

More than 20 *Salmonella* proteins are known to be translocated by the T3SS-2 across the phagosomal membrane (Srikanth *et al.*, 2011).

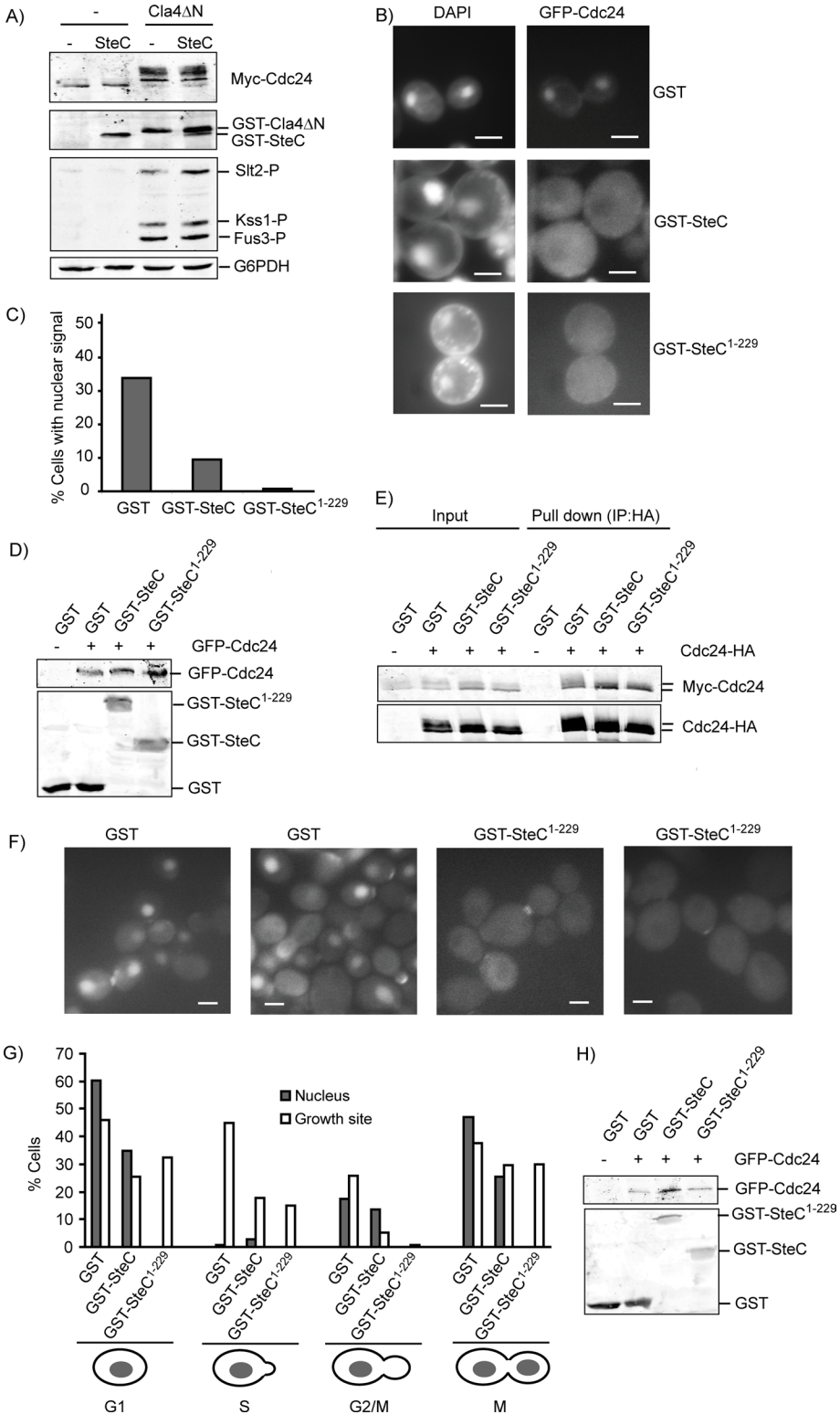

FIGURE 7: SteC modifies Cdc24 localization and does not affect Cdc24 phosphorylation and oligomerization. (A) Western blotting analysis of cell extracts from YPH499 cells harboring plasmids p414-3xmycCdc24Fl and pEG(KG) (–) or pEG(KG)-*cla4ΔN* (Cla4ΔN) and cotransformed with pEG(KG)H (–) or pEG(KG)H-SteC (SteC). Cells were grown to mid–log phase in raffinose-based selective medium, and then galactose was added for a final 2% for an additional 6 h. The 3xmycCdc24 was detected with 9E10 antibodies, and anti-G6PDH was used to detect G6PDH as a loading control. (B) Fluorescence microscopy photographs showing in vivo localization of Cdc24 and colocalization with 4′,6-diamidino-2-phenylindole staining. YKT725 cells expressing GFP-tagged Cdc24 and transformed with pEG(KG) (GST), pEG(KG)-SteC (GST-SteC), or pEG(KG)- SteC$^{1-229}$ (GST-SteC$^{1-229}$) were cultured as in A. Samples were taken at 6 h for microscope analysis. Bars, 5 μm. (C) Percentage of cells from the same cultures used in B, showing nuclear Cdc24. (D) Western blotting analysis of GFP-Cdc24 from the same cultures used in B, using anti-GFP and anti-GST antibodies. (E) RAY1773 cells expressing HA-tagged Cdc24 were cotransformed with p414-3xmycCdc24Fl plasmid and pEG(KG)H (GST), pEG(KG)H-SteC (GST-SteC), or pEG(KG) H-SteC$^{1-229}$ (GST-SteC$^{1-229}$) and cultured as in B. HA-tagged Cdc24 was immunoprecipitated from cell extracts, and bound Myc-Cdc24 was assayed by Western blotting. (F) Fluorescence microscopy photographs showing the in vivo localization of YKT725 cells cultured as in B but with samples taken at 2 h after galactose addition. Bars, 5 μm. (G) Percentage of cells showing nuclear (gray bars) or growth sites (bud tips or septa, white bars) localization of GFP-Cdc24 at different stages of the cell cycle. The indicated transformants were cultured as in F. $n > 100$ cells for each strain and for each cell cycle stage. (H) Western blotting analysis of YKT725 cell extracts of cells showed in G.

However, the specific roles of many of these effectors are far from being well understood. Unveiling their functions is hindered by the fact that bacterial effectors are often multifunctional proteins with different activities able to target many processes of eukaryotic physiology. Moreover, different effectors may display overlapping effects and cooperate to promote specific alterations in the host cell (Galan, 2009). Such redundancy could account for the absence of virulence attenuation in animal models by bacteria lacking a specific effector, as occurs with SteC (Geddes *et al.*, 2005; Poh *et al.*, 2008). These constraints have prompted the use of alternative approaches to investigate the functional roles of secreted bacterial proteins.

Here, by exploiting the yeast model, we identified a novel activity of SteC as a negative regulator of the GTPase Cdc42. Several observations support this conclusion: 1) overexpression of SteC specifically inhibits Cdc42-mediated MAPK pathways, 2) epistasis analysis places SteC at the level of Cdc42 in the mating pathway, 3) overexpression of either *S. cerevisiae* or human Cdc42 is able to counteract yeast growth inhibition caused by SteC, 4) this growth rescue is also achieved by overexpressing yeast suppressor genes of *cdc42* mutations, and 5) SteC displays a similar localization as Cdc42 in the yeast cell. A large body of work has shown that various bacterial effectors modulate the GTPase cycle either by acting as GEFs or GAPs (Orchard and Alto, 2012)

or by modifying the activity of GTPase regulators, as reported for the Rho GEF inhibitor EspH from enteropathogenic and enterohemorrhagic *E. coli* (Dong *et al.*, 2010). In the case of SteC, our data indicate that Cdc42 inhibition is likely exerted via binding to its cognate GEF. First, overexpression of SteC in yeast cannot suppress the effect of the constitutively GTP bound mutant $Cdc42^{G12V}$. Second, SteC is able to interact both in vivo and in vitro with Cdc24, the sole GEF for this GTPase in yeast, but not with Cdc42. Third, SteC also binds to the Cdc24-like GEFs *S. pombe* Scd1 and human Vav1. Fourth, cellular localization of Cdc24 is altered by SteC expression.

The effector EspH has been shown to bind directly the DH domain of multiple Rho GEFs, thus preventing their binding to Rho and thereby inhibiting nucleotide exchange–mediated Rho activation (Dong *et al.*, 2010). SteC also interacts with the DH domain of GEFs, but it is not able to inhibit in vitro the exchange capacity of Vav1, a human GEF that belongs to the Dbl family and contains a catalytic DH domain similar to yeast Cdc24. Although it is possible that our in vitro assays lacked an essential cofactor required in cells to exert the biological effect, the molecular mechanism responsible for the action of SteC on the target GEF seems to be different from that described for EspH. Inhibition of the exchange activity is not the only way to modulate GEF function in eukaryotic cells. For example, MLK3 binds to the Rho activator p63RhoGEF, impeding its activation by Gαq and thus preventing Rho activation (Swenson-Fields *et al.*, 2008). Our results suggest that alteration of Cdc24 cellular localization could account for the defect in Cdc42 functionality. Cdc24 shuttling between the nucleus and the cytoplasm regulates cell polarity (Nern and Arkowitz, 2000; Shimada *et al.*, 2000) due to its role in localizing Cdc42 at growth sites (Howell and Lew, 2012). Far1 has been shown to be responsible for nuclear sequestration of Cdc24 (Nern and Arkowitz, 2000; Shimada *et al.*, 2000). In addition, the GTPase Rsr1 seems to be involved not only in Cdc24 targeting to the growth site, but also in its activation. However, the fact that the double *far1*Δ *rsr1*Δ mutant is viable suggests that additional proteins are also involved in recruiting Cdc24 to specific sites at the cell cortex (Shimada *et al.*, 2004). Binding to SteC might inhibit the interaction of Cdc24 with any of these proteins involved in proper localization of active Cdc24. This hypothesis is consistent with our data showing that Rsr1 overexpression partially recovers the growth inhibition imposed by SteC, bearing in mind that overexpression of Rsr1 rescues the growth defect of a *cdc24* mutant unable to interact with Rsr1 (Shimada *et al.*, 2004). It is also tempting to speculate that SteC could modify Vav1 localization in human cells, since this GEF has also been shown to undergo nucleocytoplasmic redistribution (Adam *et al.*, 2000; Bertagnolo *et al.*, 2012). Additional experiments in mammalian cells are needed to test this possibility.

Expression in yeast provides a convenient way to define the functional domains of bacterial effector proteins (Aleman *et al.*, 2005). According to our results, the N-terminal region of SteC is responsible for the observed Cdc42 inhibition. The C-terminal, Raf1-homologous, kinase domain of SteC is necessary for inducing the formation of the F-actin meshwork around the *Salmonella*-containing vacuole inside host cells (Poh *et al.*, 2008). Therefore our findings suggest that SteC, as with many other bacterial effectors (Dean, 2011), is composed of functionally distinct domains conforming to a modular protein. *Salmonella* Typhimurium SipA effector is cleaved by caspase-3 within the host cell, thereby generating two independent active domains (Srikanth *et al.*, 2010). These authors also reported that other caspase-3 sites identified within *Salmonella* Typhimurium proteins appear to be restricted to T3SS translocated effectors, which indicates that proteolytic cleavage may be a strategy used by the pathogen for activating effectors delivered in a precursor form. Of interest, we found a putative caspase-3 recognition site, DXXD (spanning amino acids 205–208), located between the two functional regions of SteC. It is therefore tempting to speculate that this protein could be processed by proteolytic cleavage into two functionally independent effector peptides.

We identified SteC in a screen for *Salmonella* proteins that cause toxicity in yeast cells. Overexpression of SteC resulted in large, swollen, and unbudded cells with depolarized actin (Aleman *et al.*, 2009), resembling the phenotype described for *cdc42* or *cdc24* mutant cells (Perez and Rincon, 2010) and consistent with the Cdc42-inhibitory function of SteC described here. Thus our results suggest that not only the kinase domain, but also the N-terminal region of SteC could be modulating the actin cytoskeleton via Cdc42. This idea is in agreement with previous observations by Poh *et al.* (2008), who found that full-length SteC induced formation of F-actin clusters and cables randomly distributed throughout the cytoplasm, whereas in mammalian cells expressing the kinase domain alone, these structures were mainly found at the cell periphery. Because the Rho family of small GTPases comprises important regulators of actin organization (Hall, 1998), targeting these GTPases or their regulators is one of the most common mechanisms used by bacterial effectors to manipulate cytoskeleton pathways. The mammalian GEF Vav1 has been shown to regulate actin cytoskeleton changes associated with RhoA, Rac1, and Cdc42 (Olson *et al.*, 1996). Therefore binding of SteC to Vav1 suggests that this *Salmonella* effector could be influencing actin dynamics via Vav1. In addition, Vav1 has been reported to play a role in bacterial lipopolysaccharide-mediated macrophage activation and nitric oxide synthase production (Godambe *et al.*, 2004). The action of SteC on Vav1 would be also consistent with the function of the *Salmonella* SPI-2 in counteracting the nitrosative stress in host macrophages (Das *et al.*, 2009).

By expressing SteC in yeast, we have been able to evaluate the effect of Cdc42 function on yeast MAPK signaling. As opposed to the inhibition of the mating pathway described here, we previously reported that expression of SteC led to the activation of Slt2, the MAPK operating in the CWI pathway (Aleman *et al.*, 2009). It is likely that the morphogenetic and cell wall alterations originating from SteC-induced Cdc42 inhibition leads to a stress sensed by the CWI pathway. These results confirm that Cdc42 is not directly mediating signal transduction through the CWI pathway and underscore the role of this GTPase as a key component of the mating pathway. Because the CWI pathway is mediated by the GTPase Rho1 (Chen and Thorner, 2007), our results also point to a specificity of SteC for Cdc42 GEFs in the yeast model. Consistently, we could not detect binding of SteC to the Rho1 GEF Rom1 (Perez and Rincon, 2010). Although this GEF shares 23% identity with Cdc24 within the DH domain, other regions distinct from the DH domain of Rom1 could restrict its binding to SteC, in contrast to that occurring for Cdc24. We also show here that signaling induced by pheromone can be reduced to basal levels by interfering with the Cdc42 GEF Cdc24, emphasizing its key role not only in the morphogenetic changes associated with mating, but also in signaling through the MAPK mating pathway. Moreover, signaling inhibition caused by SteC supports the model in which two complementary signaling nodes—the Ste5-bound kinases and the Cdc42–Ste20 complex—assemble at the yeast plasma membrane to initiate activation of the mating pathway (Winters *et al.*, 2005). More broadly, our results show that expression of bacterial effectors in yeast cells can be exploited to uncover novel properties of these proteins, as well as to provide new tools to study yeast signaling.

Strain	Genotype	Source
YPH499	*MAT*a *ade2-101 trp1-63 leu2-1 ura3-52 his3-Δ200 lys2-801*	P. Hieter (British Columbia University, Vancouver, Canada)
YDM400	*MAT*a *ade2-101 trp1-63 leu2-1 ura3-52 his3-Δ200 lys2-801 sst2-Δ2*	H. Dohlman (North Carolina University, Chapel Hill, NC)
BY4741	*MAT*a *his3Δ1 leu2Δ met15Δ ura3Δ*	EUROSCARF
Y04500	*MATα his3Δ1 leu2Δ met15Δ ura3Δ, itc1::kanMX4*	EUROSCARF
Y01268	*BY4741 isogenic, far1::kanMX4*	EUROSCARF
Y02724	*BY4741 isogenic hog1::kanMX4*	EUROSCARF
Y03340	*BY4741 isogenic, ste50::kanMX4*	EUROSCARF
Y03439	*BY4741 isogenic, bem1::kanMX4*	EUROSCARF
Y03857	*BY4741 isogenic ste7::kanMX4*	EUROSCARF
Y00993	*BY4741 isogenic slt2::kanMX4*	EUROSCARF
Y06981	*BY4741 isogenic kss1::kanMX4*	EUROSCARF
Y03042	*BY4741 isogenic fus3::kanMX4*	EUROSCARF
TM141	MATa *leu2 ura3 trp1 his3*	Alonso-Monge *et al.* (2001)
TM257	MATα *ura3 leu2 trp1 his3 ssk2::LEU2 ssk22::LEU2*	Raitt *et al.* (2000)
BYgpa1	*BY4741 isogenic gpa1::kanMX4*	H. Martín (Complutense University, Madrid, Spain)
RAY1773	*MAT***a** *leu2-3,-112 ura3-52 trp1-1 ade2-1 his3-11 can1-100 GAL bar1 cdc24×3HA::Klactis URA*	Mionnet *et al.* (2008)
YKT725	*MAT***a** *cdc24Δ::KanMX6 ura3-52 his3Δ-200 trp1Δ-63 leu2Δ-1 lys2-801* pKT1154 (pRS415-Cdc24p-GFP-CDC24)	Fujimura-Kamada *et al.* (2012)

EUROSCARF, European *Saccharomyces cerevisiae* Archive for Functional Analysis, Institute for Molecular Biosciences, Johann Wolfgang Goethe-University Frankfurt, Frankfurt, Germany.

TABLE 1: *S. cerevisiae* strains used in this work.

MATERIALS AND METHODS

Bacterial and yeast strains and yeast genetics methods

The *S. cerevisiae* strains used in this study are listed in Table 1. The *Salmonella* Typhimurium SL1344 strain (Hoiseth and Stocker, 1981) used in this study was kindly provided by F. García del Portillo. The PPG103 *S. pombe* strain (h- *leu1-32 ura4-D18*) was provided by Pilar Pérez (Moreno *et al.*, 1991). Standard procedures were used for yeast genetic manipulations (Sherman, 1991). Yeast transformations were performed with the lithium acetate method (Ito *et al.*, 1983).

Culture conditions

YPD (1% yeast extract, 2% peptone, and 2% glucose) broth or agar was the complete medium used for growing the yeast strains. Synthetic medium (SD) contained 0.17% yeast nitrogen base without amino acids and ammonium sulfate, 0.5% ammonium sulfate, and 2% glucose and was supplemented with appropriate amino acids and nucleic acid bases (Sherman, 1991). SG and SR were SD with 2% galactose or raffinose, respectively, instead of glucose. Galactose induction experiments in liquid media were performed by growing cells in SR medium to log phase, then adding galactose to 2% for the indicated time. The effects of the overexpression of distinct proteins on yeast growth were tested by spotting cells onto SD or SG plates. Briefly, transformants were grown in liquid SD medium at 24°C to an OD_{600} of 0.5, and 5 µl of a 10-fold dilution series of this culture was spotted onto the indicated plates.

DNA manipulation and plasmids

General DNA methods were used, using standard techniques (Sambrook *et al.*, 1989). The *steC*-containing plasmids used in this study are described in Supplemental Table S1 and were constructed by PCR amplification from *Salmonella* Typhimurium SL1344 genomic DNA, using oligonucleotides described in Supplemental Table S2 and cloning in the correct orientation into the corresponding site of pEG(KG) (*URA3 GAL1*-GST *leu2-d* 2µ; Mitchell *et al.*, 1993). Amplified DNA was verified by DNA sequencing.

Screening for suppressors of SteC toxicity

YPH499 strain bearing plasmid YCpLG-SteC for SteC expression driven by *GAL1* promoter was transformed with a yeast cDNA library in pYES2 plasmid (kindly provided by Enrique Herrero; Espinet *et al.*, 1995) and plated on SG medium in order to select clones able to grow in the presence of galactose as carbon source and therefore able to suppress the impaired growth of SteC-expressing cells. From 128,000 clones screened, 20 were selected by this means. Twelve of them showed dependence on the pYES2-based plasmid for growing on galactose, as revealed by plasmid loss and 5-fluoroorotic acid counterselection.

Quantitative β-galactosidase assays

β-Galactosidase assays were performed as described (Hao *et al.*, 2003). Briefly, cells were transformed with plasmid pRS423-FUS1-*lacZ* for expression of β-galactosidase under the control of *FUS1* promoter as reporter for mating pathway activation. Overnight cultures were refreshed in SD medium, grown during the day, refreshed in SR medium at an OD_{600} of 0.01, and cultured overnight. Then they were refreshed in the same medium at an OD_{600} of 0.3, and galactose was added to a final concentration of 2%. After 3–4 h (OD_{600} of 0.6–0.8), 90 µl of each culture was transferred to a 96-well plate and α-factor was added to different final concentrations (0, 0.001, 0.003, 0.01, 0.03, 0.1, 0.3, 1, 3, 10, and 30 µM) in a final

volume of 100 µl. Plates were incubated at 30 °C for 90 min, and 20 µl of FDG solution (130 mM 1,4-piperazinediethanesulfonic acid, pH 7.2, 0.25% Triton X-100, 0.5 mM fluorescein-di-β-galactopyranoside) was added. Plates were incubated at 37°C for 1 h, and reaction was stopped by adding 20 µl of $NaHCO_3$, 1 M, before measuring the fluorescence signal in a PerkinElmer fluorimeter (PerkinElmer, Waltham, MA).

Preparation of yeast extracts and immunoblot analysis

The procedures used have been previously described (Martin *et al.*, 2000). Immunodetection of actin and Myc-tagged proteins was carried out using monoclonal C4 (IMP Biomedicals, Santa Ana, CA) and 9E10 (Covance, Berkeley, CA) antibodies, respectively. Anti–phospho-p44/p42 MAPK (Thr-202/Tyr-204), anti–phospho-p38 MAPK (Thr-180/Tyr-182; Cell Signaling, Beverly, MA), anti-GST (Santa Cruz Biotechnology, Santa Cruz, CA), anti-TAP (Open Biosystems, Huntsville, AL), anti-His (Sigma-Aldrich, St. Louis, MO), anti–glucose-6-phosphate dehydrogenase (G6PDH) antibodies (Sigma-Aldrich), anti-GFP Jl-8 (Clontech, Mountain View, CA) and anti-HA (Roche, Indianapolis, IN) antibodies were also used. The primary antibodies were detected either using a horseradish peroxidase–conjugated secondary antibody with the ECL detection system (Amersham, Piscataway, NJ) or a fluorescently conjugated secondary antibody with an Odyssey Infrared Imaging System (LI-COR Biosciences, Lincoln, NE).

Expression of recombinant proteins in *E. coli* and preparation of extracts

Recombinant GST- or histidine-tagged proteins were expressed from pGEX-KG or in *E. coli* strain Rosetta DE3 (Novagen, Gibbstown, NJ). Cells were collected and lysed by sonication in phosphate-buffered saline (PBS) buffer containing 2 mM phenylmethylsulfonyl fluoride, 1 mM dithiothreitol (DTT), 1 mM EDTA, and 1 mg/ml lysozyme in the presence of protease inhibitor cocktail (Roche). Extracts were clarified by centrifugation and then stored at −80°C.

Copurification assays

For in vivo binding assays, yeast cells were resuspended in lysis buffer lacking SDS and Triton X-100 and broken with glass beads in a Fast Prep machine. Samples were adjusted to a final volume of 200 µl. Then, 100 µl of 50% slurry of glutathione-Sepharose 4B resin in lysis buffer was added and incubated on a roller for 3–12 h at 4°C. Beads, recovered by brief centrifugation, were then washed five times in lysis buffer and subsequently resuspended in 30 µl of 2× SDS–PAGE sample loading buffer. Bound proteins were eluted by boiling for 10 min. After centrifugation at 13,200 rpm for 15 s, the resulting supernatant was resolved by SDS–PAGE, transferred to nitrocellulose, and processed for immunoblotting. For in vivo binding assays to Gpa1, yeast cells were resuspended in 250 µl of the corresponding lysis buffer (40 mM triethanolamine, pH 7.2, 2 mM EDTA, 150 mM NaCl, 2 mM DTT, 3 mM $MgCl_2$, and protease inhibitors) and broken with glass beads in a Fast Prep machine. Lysates were cleared by centrifugation at 3200 rpm twice for 10 min each, and 1.5% Triton X-100 was added to the resulting supernatant solution for 1 h. Then the insoluble material was removed by centrifugation at 13,200 rpm for 10 min. Samples were then processed in the same way as described previously.

In vitro binding assays were performed by binding GST or GST-fused proteins from *E. coli* extracts to glutathione-Sepharose 4B resin, and then either *E. coli* or yeast extracts bearing the corresponding tagged proteins were added and processed as described.

Immunoprecipitation assays

To analyze Cdc24 oligomerization, RAY1773 yeast cells expressing HA-tagged Cdc24 transformed with p414-3xmycCdc24Fl plasmid for expression of myc-tagged Cdc24 and pEG(KG)H, pEG(KG)H-SteC, or pEG(KG)H-$SteC^{1-229}$ were lysed in the same buffer used in copurification assays. Dynabeads PanMouse immunoglobulin G (Invitrogen, Carlsbad, CA), 25 µl/sample, was incubated with anti-HA.11 antibody (clone 16B12; Covance) at a dilution of 1:150 for 2–3 h at 4°C. After washing with PBS and 0.1% bovine serum albumin, cell extracts were added and the mixture was incubated for 3–4 h. Then, beads were washed three times, eluted by boiling in 30 µl of 2× SDS–PAGE sample loading buffer, and assayed by Western blotting with anti-myc and anti-HA antibodies.

Guanine nucleotide exchange assays

In vitro guanine nucleotide exchange was carried out essentially as described previously (Rojas *et al.*, 2003). For loading reactions, 400 nM Rac1 and 80 nM Bodipy FL GDP were incubated in 1 ml of buffer consisting of 20 mM Tris, pH 7.5, 150 mM NaCl, 5 mM $MgCl_2$, 5% (vol/vol) glycerol, 2 mM DTT, and 0.08% (vol/vol) NP-40, and fluorescence (λ_{ex} = 502 nm; λ_{em} = 511 nm) was monitored with a PerkinElmer LS55 spectrofluorometer (slits, 2.5 nm) thermostatted to 15°C. At the indicated time, 4 µl of a stock solution consisting of 1.25 µM Vav1 (DH/PH/CRD fragment; Chrencik *et al.*, 2008) either alone or preincubated for 5 min with 12.5 µM SteC, was added, resulting in final concentrations of 5 nM Vav1 and 50 nM SteC. Unloading reactions were carried out similarly, except that Rac1 was preloaded with Bodipy FL GDP and incubated with 20 µM GDP before additions of Vav1 and SteC, resulting in final concentrations of 10 and 100 nM, respectively.

Microscopy and immunofluorescence

Fluorescence microscopy of live yeast cells for GFP detection was performed as described (Rodriguez-Escudero *et al.*, 2006). Cells harboring GFP fusion vectors with *MET25* promoter were cultured overnight in selective SD medium and then washed three times with sterile water and refreshed in the same medium lacking methionine. After 6 h at 30°C cell suspensions were spotted on slides for microscopy observation. For FM4-64 staining, cells were pelleted, resuspended in the same medium containing 40 µM FM4-64, and incubated for 1 h at 30°C. Differential interference contrast (DIC) images were acquired by using an Eclipse TE2000U microscope (Nikon, Melville, NY) fitted with an Orca C4742-95-12ER digital camera (Hamamatsu, Hamamatsu, Japan) and then processed by using Aquacosmos Imaging System software (Hamamatsu).

ACKNOWLEDGMENTS

We thank Pilar Pérez, Francisco García del Portillo, Enrique Herrero, Peter Pryciak, Benjamin Rhau, Kazuma Tanaka, Daniel Lew, Douglas Johnson, Francesc Posas, Scott Emr, and Robert A. Arkowitz for providing reagents; Janeen Vanhooke and Dan Isom for technical assistance; and Víctor J. Cid, Rafael Rotger, Federico Mayor, and Cristina Murga for helpful discussion. The research was supported by Grants BIO2007-67299 and BIO2010-22369-C02-01 from Ministerio de Ciencia e Innovación (Spain), PROMPT S2010/BMD-2414 from Comunidad Autónoma de Madrid (Spain), and the Program for UCM Research Groups (920628) from Banco Santander Central Hispano–Universidad Complutense de Madrid to M.M. P.F-P. was the recipient of a predoctoral fellowship from Fundación Ramón Areces (Spain).

REFERENCES

Adam L, Bandyopadhyay D, Kumar R (2000). Interferon-alpha signaling promotes nucleus-to-cytoplasmic redistribution of p95Vav, and formation of a multisubunit complex involving Vav, Ku80, and Tyk2. Biochem Biophys Res Commun 267, 692–696.

Aleman A, Fernandez-Pinar P, Perez-Nunez D, Rotger R, Martin H, Molina M (2009). A yeast-based genetic screen for identification of pathogenic *Salmonella* proteins. FEMS Microbiol Lett 296, 167–177.

Aleman A, Rodriguez-Escudero I, Mallo GV, Cid VJ, Molina M, Rotger R (2005). The amino-terminal non-catalytic region of *Salmonella typhimurium* SigD affects actin organization in yeast and mammalian cells. Cell Microbiol 7, 1432–1446.

Alonso-Monge R, Real E, Wojda I, Bebelman JP, Mager WH, Siderius M (2001). Hyperosmotic stress response and regulation of cell wall integrity in *Saccharomyces cerevisiae* share common functional aspects. Mol Microbiol 41, 717–730.

Andersson J, Simpson DM, Qi M, Wang Y, Elion EA (2004). Differential input by Ste5 scaffold and Msg5 phosphatase route a MAPK cascade to multiple outcomes. EMBO J 23, 2564–2576.

Apanovitch DM, Slep KC, Sigler PB, Dohlman HG (1998). Sst2 is a GTPase-activating protein for Gpa1: purification and characterization of a cognate RGS-Galpha protein pair in yeast. Biochemistry 37, 4815–4822.

Bakowski MA, Braun V, Brumell JH (2008). *Salmonella*-containing vacuoles: directing traffic and nesting to grow. Traffic. 9, 2022–2031.

Bertagnolo V, Brugnoli F, Grassilli S, Nika E, Capitani S (2012). Vav1 in differentiation of tumoral promyelocytes. Cell Signal 24, 612–620.

Bose I, Irazoqui JE, Moskow JJ, Bardes ES, Zyla TR, Lew DJ (2001). Assembly of scaffold-mediated complexes containing Cdc42p, the exchange factor Cdc24p, and the effector Cla4p required for cell cycle-regulated phosphorylation of Cdc24p. J Biol Chem 276, 7176–7186.

Caffrey DR, O'Neill LA, Shields DC (1999). The evolution of the MAP kinase pathways: coduplication of interacting proteins leads to new signaling cascades. J Mol Evol 49, 567–582.

Chakravortty D, Hansen-Wester I, Hensel M (2002). *Salmonella* pathogenicity island 2 mediates protection of intracellular *Salmonella* from reactive nitrogen intermediates. J Exp Med 195, 1155–1166.

Chen RE, Thorner J (2007). Function and regulation in MAPK signaling pathways: lessons learned from the yeast *Saccharomyces cerevisiae*. Biochim Biophys Acta 1773, 1311–1340.

Chrencik JE *et al*. (2008). Structural basis of guanine nucleotide exchange mediated by the T-cell essential Vav1. J Mol Biol 380, 828–843.

Cole GM, Stone DE, Reed SI (1990). Stoichiometry of G protein subunits affects the Saccharomyces cerevisiae mating pheromone signal transduction pathway. Mol Cell Biol 10, 510–517.

Cote P, Sulea T, Dignard D, Wu C, Whiteway M (2011). Evolutionary reshaping of fungal mating pathway scaffold proteins. MBio 2, e00230-10.

Das P, Lahiri A, Lahiri A, Chakravortty D (2009). Novel role of the nitrite transporter NirC in *Salmonella* pathogenesis: SPI2-dependent suppression of inducible nitric oxide synthase in activated macrophages. Microbiology 155, 2476–2489.

Dean P (2011). Functional domains and motifs of bacterial type III effector proteins and their roles in infection. FEMS Microbiol Rev 35, 1100–1125.

Dohlman HG, Apaniesk D, Chen Y, Song J, Nusskern D (1995). Inhibition of G-protein signaling by dominant gain-of-function mutations in Sst2p, a pheromone desensitization factor in *Saccharomyces cerevisiae*. Mol Cell Biol 15, 3635–3643.

Dohlman HG, Slessareva JE (2006). Pheromone signaling pathways in yeast. Sci STKE 2006, cm6.

Dong N, Liu L, Shao F (2010). A bacterial effector targets host DH-PH domain RhoGEFs and antagonizes macrophage phagocytosis. EMBO J 29, 1363–1376.

Drogen F, O'Rourke SM, Stucke VM, Jaquenoud M, Neiman AM, Peter M (2000). Phosphorylation of the MEKK Ste11p by the PAK-like kinase Ste20p is required for MAP kinase signaling in vivo. Curr Biol 10, 630–639.

Espinet C, de la Torre MA, Aldea M, Herrero E (1995). An efficient method to isolate yeast genes causing overexpression-mediated growth arrest. Yeast 11, 25–32.

Feig LA (1999). Tools of the trade: use of dominant-inhibitory mutants of Ras-family GTPases. Nat Cell Biol 1, E25–E27.

Fujimura-Kamada K, Hirai T, Tanaka K (2012). Essential role of the NH2-terminal region of Cdc24 guanine nucleotide exchange factor in its initial polarized localization in *Saccharomyces cerevisiae*. Eukaryot Cell 11, 2–15.

Galan JE (2009). Common themes in the design and function of bacterial effectors. Cell Host Microbe 5, 571–579.

Galan JE, Wolf-Watz H (2006). Protein delivery into eukaryotic cells by type III secretion machines. Nature 444, 567–573.

Geddes K, Worley M, Niemann G, Heffron F (2005). Identification of new secreted effectors in *Salmonella* enterica serovar *typhimurium*. Infect Immun 73, 6260–6271.

Godambe SA, Knapp KM, Meals EA, English BK (2004). Role of vav1 in the lipopolysaccharide-mediated upregulation of inducible nitric oxide synthase production and nuclear factor for interleukin-6 expression activity in murine macrophages. Clin Diagn Lab Immunol 11, 525–531.

Gulli MP, Jaquenoud M, Shimada Y, Niederhauser G, Wiget P, Peter M (2000). Phosphorylation of the Cdc42 exchange factor Cdc24 by the PAK-like kinase Cla4 may regulate polarized growth in yeast. Mol Cell 6, 1155–1167.

Hall A (1998). Rho GTPases and the actin cytoskeleton. Science 279, 509–514.

Hao N, Yildirim N, Wang Y, Elston TC, Dohlman HG (2003). Regulators of G protein signaling and transient activation of signaling: experimental and computational analysis reveals negative and positive feedback controls on G protein activity. J Biol Chem 278, 46506–46515.

Heasman SJ, Ridley AJ (2008). Mammalian Rho GTPases: new insights into their functions from in vivo studies. Nat Rev Mol Cell Biol 9, 690–701.

Hoiseth SK, Stocker BA (1981). Aromatic-dependent *Salmonella typhimurium* are non-virulent and effective as live vaccines. Nature 291, 238–239.

Howell AS, Lew DJ (2012). Morphogenesis and the cell cycle. Genetics 190, 51–77.

Irie K, Gotoh Y, Yashar BM, Errede B, Nishida E, Matsumoto K (1994). Stimulatory effects of yeast and mammalian 14-3-3 proteins on the Raf protein kinase. Science 265, 1716–1719.

Ito H, Fukuda Y, Murata K, Kimura A (1983). Transformation of intact yeast cells treated with alkali cations. J Bacteriol 153, 163–168.

Kozminski KG, Beven L, Angerman E, Tong AH, Boone C, Park HO (2003). Interaction between a Ras and a Rho GTPase couples selection of a growth site to the development of cell polarity in yeast. Mol Biol Cell 14, 4958–4970.

Kozminski KG, Chen AJ, Rodal AA, Drubin DG (2000). Functions and functional domains of the GTPase Cdc42p. Mol Biol Cell 11, 339–354.

Lazer G, Katzav S (2011). Guanine nucleotide exchange factors for RhoGTPases: good therapeutic targets for cancer therapy? Cell Signal. 23, 969–979.

Ly KT, Casanova JE (2007). Mechanisms of *Salmonella* entry into host cells. Cell Microbiol 9, 2103–2111.

Martin H, Mendoza A, Rodriguez-Pachon JM, Molina M, Nombela C (1997). Characterization of SKM1, a *Saccharomyces cerevisiae* gene encoding a novel Ste20/PAK-like protein kinase. Mol Microbiol 23, 431–444.

Martin H, Rodriguez-Pachon JM, Ruiz C, Nombela C, Molina M (2000). Regulatory mechanisms for modulation of signaling through the cell integrity Slt2-mediated pathway in *Saccharomyces cerevisiae*. J Biol Chem 275, 1511–1519.

McGhie EJ, Brawn LC, Hume PJ, Humphreys D, Koronakis V (2009). *Salmonella* takes control: effector-driven manipulation of the host. Curr Opin Microbiol 12, 117–124.

Meresse S, Unsworth KE, Habermann A, Griffiths G, Fang F, Martinez-Lorenzo MJ, Waterman SR, Gorvel JP, Holden DW (2001). Remodelling of the actin cytoskeleton is essential for replication of intravacuolar *Salmonella*. Cell Microbiol 3, 567–577.

Mionnet C, Bogliolo S, Arkowitz RA (2008). Oligomerization regulates the localization of Cdc24, the Cdc42 activator in *Saccharomyces cerevisiae*. J Biol Chem 283, 17515–17530.

Mitchell DA, Marshall TK, Deschenes RJ (1993). Vectors for the inducible overexpression of glutathione S-transferase fusion proteins in yeast. Yeast 9, 715–722.

Moreno S, Klar A, Nurse P (1991). Molecular genetic analysis of fission yeast *Schizosaccharomyces pombe*. Methods Enzymol 194, 795–823.

Munemitsu S, Innis MA, Clark R, McCormick F, Ullrich A, Polakis P (1990). Molecular cloning and expression of a G25K cDNA, the human homolog of the yeast cell cycle gene CDC42. Mol Cell Biol 10, 5977–5982.

Nern A, Arkowitz RA (2000). Nucleocytoplasmic shuttling of the Cdc42p exchange factor Cdc24p. J Cell Biol 148, 1115–1122.

O'Rourke SM, Herskowitz I (1998). The Hog1 MAPK prevents cross talk between the HOG and pheromone response MAPK pathways in *Saccharomyces cerevisiae*. Genes Dev 12, 2874–2886.

Ohl ME, Miller SI (2001). *Salmonella*: a model for bacterial pathogenesis. Annu Rev Med 52, 259–274.
Olson MF, Pasteris NG, Gorski JL, Hall A (1996). Faciogenital dysplasia protein (FGD1) and Vav, two related proteins required for normal embryonic development, are upstream regulators of Rho GTPases. Curr Biol 6, 1628–1633.
Orchard RC, Alto NM (2012). Mimicking GEFs: a common theme for bacterial pathogens. Cell Microbiol 14, 10–18.
Perez P, Rincon SA (2010). Rho GTPases: regulation of cell polarity and growth in yeasts. Biochem J 426, 243–253.
Poh J, Odendall C, Spanos A, Boyle C, Liu M, Freemont P, Holden DW (2008). SteC is a *Salmonella* kinase required for SPI-2-dependent F-actin remodelling. Cell Microbiol 10, 20–30.
Pryciak PM, Huntress FA (1998). Membrane recruitment of the kinase cascade scaffold protein Ste5 by the Gbetagamma complex underlies activation of the yeast pheromone response pathway. Genes Dev 12, 2684–2697.
Raitt DC, Posas F, Saito H (2000). Yeast Cdc42 GTPase and Ste20 PAK-like kinase regulate Sho1-dependent activation of the Hog1 MAPK pathway. EMBO J 19, 4623–4631.
Raman M, Chen W, Cobb MH (2007). Differential regulation and properties of MAPKs. Oncogene 26, 3100–3112.
Ramer SW, Davis RW (1993). A dominant truncation allele identifies a gene, STE20, that encodes a putative protein kinase necessary for mating in *Saccharomyces cerevisiae*. Proc Natl Acad Sci USA 90, 452–456.
Rapley J, Tybulewicz VL, Rittinger K (2008). Crucial structural role for the PH and C1 domains of the Vav1 exchange factor. EMBO Rep 9, 655–661.
Rodriguez-Escudero I, Ferrer NL, Rotger R, Cid VJ, Molina M (2011). Interaction of the *Salmonella typhimurium* effector protein SopB with host cell Cdc42 is involved in intracellular replication. Mol Microbiol 80, 1220–1240.
Rodriguez-Escudero I, Hardwidge PR, Nombela C, Cid VJ, Finlay BB, Molina M (2005). Enteropathogenic *Escherichia coli* type III effectors alter cytoskeletal function and signalling in *Saccharomyces cerevisiae*. Microbiology 151, 2933–2945.
Rodriguez-Escudero I, Rotger R, Cid VJ, Molina M (2006). Inhibition of Cdc42-dependent signalling in *Saccharomyces cerevisiae* by phosphatase-dead SigD/SopB from *Salmonella typhimurium*. Microbiology 152, 3437–3452.
Rodriguez-Pachon JM, Martin H, North G, Rotger R, Nombela C, Molina M (2002). A novel connection between the yeast Cdc42 GTPase and the Slt2-mediated cell integrity pathway identified through the effect of secreted *Salmonella* GTPase modulators. J Biol Chem 277, 27094–27102.
Rojas RJ, Kimple RJ, Rossman KL, Siderovski DP, Sondek J (2003). Established and emerging fluorescence-based assays for G-protein function: Ras-superfamily GTPases. Comb Chem High Throughput Screen 6, 409–418.
Rossman KL, Der CJ, Sondek J (2005). GEF means go: turning on RHO GTPases with guanine nucleotide-exchange factors. Nat Rev Mol Cell Biol 6, 167–180.
Ruiz C, Escribano MV, Morgado E, Molina M, Mazón MJ (2003). Cell-type-dependent repression of yeast a-specific genes requires Itc1p, a subunit of the Isw2p-Itc1p chromatin remodelling complex. Microbiology 149, 341–51.
Sambrook J, Fritsch EF, Maniatis T (1989). Molecular Cloning: A Laboratory Manual, Cold Spring Harbor, NY: Cold Spring Harbor Laboratory Press.
Schroeder N, Mota LJ, Meresse S (2011). *Salmonella*-induced tubular networks. Trends Microbiol 19, 268–277.
Sherman F (1991). Getting started with yeast. Methods Enzymol 194, 3–21.
Shimada Y, Gulli MP, Peter M (2000). Nuclear sequestration of the exchange factor Cdc24 by Far1 regulates cell polarity during yeast mating. Nat Cell Biol 2, 117–124.
Shimada Y, Wiget P, Gulli MP, Bi E, Peter M (2004). The nucleotide exchange factor Cdc24p may be regulated by auto-inhibition. EMBO J 23, 1051–1062.
Srikanth CV, Mercado-Lubo R, Hallstrom K, McCormick BA (2011). *Salmonella* effector proteins and host-cell responses. Cell Mol Life Sci 68, 3687–3697.
Srikanth CV, Wall DM, Maldonado-Contreras A, Shi HN, Zhou D, Demma Z, Mumy KL, McCormick BA (2010). *Salmonella* pathogenesis and processing of secreted effectors by caspase-3. Science 330, 390–393.
Steele-Mortimer O (2008). The *Salmonella*-containing vacuole: moving with the times. Curr Opin Microbiol 11, 38–45.
Stefan CJ, Audhya A, Emr SD (2002). The yeast synaptojanin-like proteins control the cellular distribution of phosphatidylinositol (4,5)-bisphosphate. Mol Biol Cell 13, 542–557.
Stevenson BJ, Rhodes N, Errede B, Sprague GF Jr (1992). Constitutive mutants of the protein kinase STE11 activate the yeast pheromone response pathway in the absence of the G protein. Genes Dev 6, 1293–1304.
Strahl T, Thorner J (2007). Synthesis and function of membrane phosphoinositides in budding yeast, *Saccharomyces cerevisiae*. Biochim Biophys Acta 1771, 353–404.
Swenson-Fields KI, Sandquist JC, Rossol-Allison J, Blat IC, Wennerberg K, Burridge K, Means AR (2008). MLK3 limits activated Galphaq signaling to Rho by binding to p63RhoGEF. Mol Cell 32, 43–56.
Toenjes KA, Sawyer MM, Johnson DI (1999). The guanine-nucleotide-exchange factor Cdc24p is targeted to the nucleus and polarized growth sites. Curr Biol 9, 1183–1186.
Truckses DM, Bloomekatz JE, Thorner J (2006). The RA domain of Ste50 adaptor protein is required for delivery of Ste11 to the plasma membrane in the filamentous growth signaling pathway of the yeast *Saccharomyces cerevisiae*. Mol Cell Biol 26, 912–928.
Truman AW, Millson SH, Nuttall JM, King V, Mollapour M, Prodromou C, Pearl LH, Piper PW (2006). Expressed in the yeast *Saccharomyces cerevisiae*, human ERK5 is a client of the Hsp90 chaperone that complements loss of the Slt2p (Mpk1p) cell integrity stress-activated protein kinase. Eukaryot Cell 5, 1914–1924.
Valdivia RH (2004). Modeling the function of bacterial virulence factors in *Saccharomyces cerevisiae*. Eukaryot Cell 3, 827–834.
Vida TA, Emr SD (1995). A new vital stain for visualizing vacuolar membrane dynamics and endocytosis in yeast. J Cell Biol 128, 779–792.
Winters MJ, Lamson RE, Nakanishi H, Neiman AM, Pryciak PM (2005). A membrane binding domain in the ste5 scaffold synergizes with gbetagamma binding to control localization and signaling in pheromone response. Mol Cell 20, 21–32.
Yakir-Tamang L, Gerst JE (2009). A phosphatidylinositol-transfer protein and phosphatidylinositol-4-phosphate 5-kinase control Cdc42 to regulate the actin cytoskeleton and secretory pathway in yeast. Mol Biol Cell 20, 3583–3597.